

Spin-wave spectrum of a superlattice with antiferromagnetic interfacial coupling

J. G. LePage and R. E. Camley

Department of Physics, University of Colorado, Colorado Springs, Colorado 80907

(Received 10 April 1989; revised manuscript received 10 July 1989)

We investigate the spin-wave spectrum of a superlattice composed of two alternating ferromagnetic films with antiferromagnetic coupling at the interfaces. Depending on the value of temperature and of an externally applied magnetic field, this system can exist in any of four distinct phases. The temperature- and field-dependent behaviors of the spin-wave modes in three of these phases are investigated. Propagation both perpendicular and parallel to the layers is considered. The frequency of one mode is found to increase with increasing temperature, in contradiction to the usual expectation; this behavior is explained in terms of a ferrimagnet analogy.

I. INTRODUCTION

Superlattices are interesting for two main reasons. First, since the manufacture of quality samples has only recently become possible, superlattices have not yet been subjected to the sort of intense scrutiny that has been directed towards simpler structures. As such, their properties are still somewhat unknown. The characteristics of a superlattice may be very different from those of its component materials. In fact, such crystals may exhibit behavior that is strikingly different from the typical behavior of simple solids. For instance, if the voltage applied across most semiconductors is increased, the current will increase. On the other hand, a superlattice composed of alternating layers of two different semiconductors can react to an increase in voltage with a *decrease* in current. Furthermore, unlike other negative resistance devices, such a superlattice would react to changes in voltage almost instantaneously.¹

Second, since superlattices are by necessity manmade, their structures are subject to design. Furthermore, since macroscopic properties reflect microscopic details, the behavior of these crystals can, in a sense, be specified. For a magnetic superlattice, this means that the spin-wave modes, for instance, can be varied in a *predictable* way by making changes in the superlattice architecture; even a small change, such as the addition of a single layer to a film, can result in a large quantitative variation in the characteristics of the material.

Under the general heading of magnetic superlattices can be found a wide variety of intriguing structures. Beyond the immediate combination of a superlattice whose components exhibit the same type of magnetic behavior (e.g., a superlattice composed of alternating films of different ferromagnets²), there are a variety of more interesting possibilities. For instance, a superlattice may be composed of alternating films of ferromagnetic and antiferromagnetic materials. Such a system has, in fact, been studied theoretically by Hinchey and Mills.³ Another possible system is one in which the type of magnetic interaction within both films is the same while the interaction at the interfaces between films is of a different type.⁴⁻⁷ The nature of the spin waves that travel

through this sort of structure is the focus of this paper.

In the particular superlattice analyzed here, each film is composed of ferromagnetic materials, but the interaction at the interfaces is antiferromagnetic. This sort of behavior has been experimentally observed in thin films of gadolinium formed on iron substrates⁸ and is a general feature of combinations of transition metals and rare-earth metals.⁹ The specific model analyzed in this paper is made up of alternating films of ferromagnetic materials (hereafter referred to as materials *A* and *B*) arranged in a body-centered cubic structure. For the purposes of numerical calculations, material *A* will be considered to have a moment of $\frac{5}{2}$ while material *B* will have a moment of $\frac{7}{2}$. The coordinate system is constructed so that the *y* axis is perpendicular to the interfaces between the different films, and the *z* axis lies parallel to an externally applied magnetic field. Depending on the temperature and size of the external magnetic field, such a system can exist in any of four distinct spin configurations. The static properties of this model were discussed earlier.¹⁰ The first of these spin configurations is the *B*-aligned state, in which the *B* spins are parallel to the applied magnetic field while the *A* spins are antiparallel. The system may also exist in a twisted state in which all spins are rotated in the *x-z* plane away from the *z* axis. (In the absence of anisotropy fields, there are no static configurations in which the spins are not totally within the *x-z* plane. The spins do not rotate out of this plane because that would set up static demagnetizing fields.) There is another aligned state in which the *A* spins are parallel to the external field while the *B* spins are antiparallel. Finally, there are paramagnetic phases in which some interior spins in the *B* films act essentially paramagnetically. We note that transitions from aligned states to twisted states have been observed recently in Gd/Co superlattices.¹¹

In this paper we will discuss the dynamic magnon modes which exist in the aligned and twisted states. We will find that changes in temperature and magnetic field strength result in changes in both the frequency of a mode and the shape of the wave form associated with it. Interestingly, certain superlattice magnon modes display temperature- and field-dependent behaviors that are distinctly dissimilar to the behavior of modes that exist in

simple crystals. For instance, one superlattice mode increases in frequency as temperature increases. Normally one would expect a decrease in frequency as temperature increased, because, as temperature increases, the spin magnitudes *decrease*. This, in turn, causes a decrease in the effective field at each site. The net effect is to reduce the torques acting on the spins. Naturally, one would expect frequency to decrease. And yet, for this mode, the reverse is true. This apparent contradiction can be successfully explained in terms of the superlattice architecture and the shape of the magnon wave form. Furthermore, other important features of the system can also be explained in terms of magnon character. For instance, the relative frequencies of the modes can usually be deduced from a simple inspection of the associated wave forms.

The field-dependent behaviors of some modes are also interesting. For instance, at $kL=0$ in the twisted phase, one of the lower modes is essentially field independent. This is surprising; modes are usually quite sensitive to an external magnetic field since a change in this applied field changes the effective field at each spin site. These and other unusual temperature- and field-dependent behaviors will be the primary focus of this paper.

II. THEORY

The equilibrium configuration of the system is determined through the use of a simple iterative process.¹⁰ Given the initial spin magnitudes at each site, the energy of an arbitrary spin is calculated at $T=0$ as follows:

$$\epsilon = -\mathbf{S}_n \cdot \mathbf{H}_{\text{eff},n}, \quad (1)$$

where N is the number of layers in the superlattice unit cell, and \mathbf{S}_n is the spin vector in layer n . For a body-centered cubic structure where each site has a total of eight nearest neighbors,

$$\mathbf{H}_{\text{eff},n} = 4J_{n-1,n}\mathbf{S}_{n-1} + 4J_{n,n+1}\mathbf{S}_{n+1} + \mathbf{H}_0 \quad (2)$$

is the effective field (in the nearest-neighbor approximation) that acts on a spin \mathbf{S}_n in the n th layer of the superlattice unit cell. $J_{n,n+1}$ is the exchange constant acting between layers n and $n+1$. (For ease of notation, we use J in this paper to represent the true exchange constant divided by $g\mu_B$. Thus JS has units of magnetic field.) \mathbf{H}_0 is an externally applied field which always acts along the positive z direction. We assume that the equilibrium magnitudes and directions of the spins in the zeroth layer of the superlattice are the same as those of the spins in the N th layer, and, conversely, the equilibrium magnitudes and directions of the spins in the $(N+1)$ th layer are the same as those in the first layer. To lower the energy, the spin \mathbf{S}_n is rotated to lie parallel to its effective field. A new layer of spins is then chosen and rotated into its effective field. This process continues until a self-consistent stable state emerges. Through this simple technique, the minimum energy state is determined. For finite temperatures, the procedure is changed so that after

the spins are rotated into the effective field the magnitudes of the spins are replaced by their thermal averaged values.

Given the static configuration of the system, it is a simple matter to determine the spin-wave modes. We first consider the spin-wave modes in the aligned states. The equations of motion for a spin in layer n are given by the Bloch equations:

$$\frac{d\mathbf{S}_n}{dt} = \gamma \mathbf{S}_n \times \mathbf{H}_{\text{eff},n}, \quad (3)$$

where $\gamma = g\mu_B/\hbar$ is the gyromagnetic ratio. With a time dependence of the form $e^{-i\omega t}$, the linearized equations of motion are

$$\begin{aligned} -\frac{i\omega}{\gamma} S_1^x &= S_1^y (4J_{0,1} S_0^z + 4J_{1,2} S_2^z + H_0) \\ &\quad - S_1^z (4J_{0,1} S_0^y + 4J_{1,2} S_2^y), \\ -\frac{i\omega}{\gamma} S_1^y &= S_1^z (4J_{0,1} S_0^x + 4J_{1,2} S_2^x) \\ &\quad - S_1^x (4J_{0,1} S_0^z + 4J_{1,2} S_2^z + H_0), \\ &\quad \vdots \\ -\frac{i\omega}{\gamma} S_N^x &= S_N^y (4J_{N-1,N} S_{N-1}^z + 4J_{N,N+1} S_{N+1}^z + H_0) \\ &\quad - S_N^z (4J_{N-1,N} S_{N-1}^y + 4J_{N,N+1} S_{N+1}^y), \\ -\frac{i\omega}{\gamma} S_N^y &= S_N^z (4J_{N-1,N} S_{N-1}^x + 4J_{N,N+1} S_{N+1}^x) \\ &\quad - S_N^x (4J_{N-1,N} S_{N-1}^z + 4J_{N,N+1} S_{N+1}^z + H_0). \end{aligned} \quad (4)$$

Clearly the spins inside a unit cell (sites 1 to N) are coupled to the spins in adjacent cells by the presence of terms such as $S_0^x, S_{N+1}^x, S_0^y, S_{N+1}^y, S_0^z,$ and S_{N+1}^z .

We have already assumed that the z components obey simple periodic boundary conditions. The fluctuating x and y components for spins in adjoining unit cells are related by the Bloch theorem: $\mathbf{S}_{n+N} = \mathbf{S}_n e^{ikL}$, where L is the length of the unit cell in the y direction (the direction perpendicular to the film interfaces). Thus, we can restrict the equations of motion to deal with spins in one unit cell only. We then obtain an eigenvalue equation of the form

$$\mathbf{A}\mathbf{x} = (-i\omega)\mathbf{x}, \quad (5)$$

where \mathbf{x} is a vector of length $2N$ with components $(S_1^x, S_1^y, \dots, S_N^x, S_N^y)$. For the case of the aligned states one can form linear combination $S^+ = S^x + iS^y$ and reduce the size of the matrix A and vector \mathbf{x} to a $N \times N$ matrix and a vector of length N , respectively. For the same reason, the precession of the spin vectors is always circular in the aligned states.

For the twisted states, the method outlined above must be altered slightly. However, the necessary alteration is conceptually simple. The static configuration for each spin site is given as a magnitude and an angle of rotation θ from the applied field direction in the x - z plane. Each spin site is given a local z' axis which corresponds to the orientation of its static configuration vector. θ_p is the an-

gle of rotation of the z' axis at site p from the external z axis. The y axis remains unchanged; it is always the axis perpendicular to the superlattice interfaces. The local x' axis is defined within the framework of these conventions. The equations of motion for each site are calculated with this in mind. In practice, this merely means that the effective field for site p is calculated using the components of spin $p-1$, spin $p+1$, and the external field H_0 which lie along the axes of the local coordinate system of site p . To elaborate, the effective field at site p would be given as

$$\begin{aligned} H_{\text{eff},p}^{x'} = & H_0 \sin(\theta_p) + 4J_{p,p+1} S_{p+1}^{z'} \sin(\theta_p - \theta_{p+1}) \\ & + 4J_{p,p-1} S_{p-1}^{z'} \sin(\theta_p - \theta_{p-1}) \\ & + 4J_{p,p-1} S_{p-1}^{x'} \cos(\theta_p - \theta_{p-1}) \\ & + 4J_{p,p+1} S_{p+1}^{x'} \cos(\theta_{p+1} - \theta_p), \end{aligned} \quad (6)$$

$$H_{\text{eff},p}^y = 4J_{p,p+1} S_{p+1}^y + 4J_{p,p-1} S_{p-1}^y, \quad (7)$$

$$\begin{aligned} H_{\text{eff},p}^{z'} = & H_0 \cos \theta_p + 4J_{p,p+1} S_{p+1}^{z'} \sin(\theta_{p+1} - \theta_p) \\ & + 4J_{p,p-1} S_{p-1}^{z'} \sin(\theta_{p-1} - \theta_p) \\ & + 4J_{p,p-1} S_{p-1}^{z'} \cos(\theta_p - \theta_{p-1}) \\ & + 4J_{p,p+1} S_{p+1}^{z'} \cos(\theta_{p+1} - \theta_p). \end{aligned} \quad (8)$$

$$\begin{aligned} -\frac{i\omega}{\gamma} S_p^y = & S_p^{z'} [4J_{p,p+1} S_{p+1}^{x'} \cos(\theta_{p+1} - \theta_p) + 4J_{p,p-1} S_{p-1}^{x'} \cos(\theta_p - \theta_{p-1})] \\ & - S_p^{x'} [H_0 \cos \theta_p + 4J_{p,p+1} S_{p+1}^{z'} \cos(\theta_{p+1} - \theta_p) + 4J_{p,p-1} S_{p-1}^{z'} \cos(\theta_p - \theta_{p-1})]. \end{aligned} \quad (12)$$

These are similar to the equations we obtained for the aligned system; the only difference is the presence of the cosine terms. Again we use Bloch's theorem in order to restrict the spin variables to one unit cell and obtain an eigenvalue equation.

For the purposes of the numerical calculations, we take the same values as in Ref. 10. Thus $J_B/J_A = 0.155$ and $J_{\text{interface}}/J_A = -1$. The external field magnitude is given in units of $J_A/g\mu_B$, where J_A is the true exchange constant. In Ref. 10, which is concerned with the static configuration of this system, the external field magnitude was given in units of $J_A S_A/g\mu_B$, where S_A is the value of the A spin vector at $T=0.0$. The temperature is given in terms of the reduced temperature:

$$t = \frac{T_{\text{abs}}}{T_{\text{Curie}, A}}. \quad (13)$$

T_{Curie} is related to J , in the mean-field case, by the usual relation

$$J = \frac{3k_B T_{\text{Curie}}}{2zS(S+1)}. \quad (14)$$

In Eq. 14, J is the true exchange constant. Note that the Curie temperature of material A is much higher than the Curie temperature of material B ($T_{c,A} = 3.57T_{c,B}$). The frequency ω is given in units of J_A/\hbar , where J_A is the true exchange constant. In this paper, γ is set equal to unity.

Note that the first three terms of Eq. (6) are static quantities. However, the static field along the x' and y' axes must always be zero because the z' axis is always aligned with the static field. Thus,

$$\begin{aligned} H_0 \sin(\theta_p) + 4J_{p,p+1} S_{p+1}^{z'} \sin(\theta_p - \theta_{p+1}) \\ + 4J_{p,p-1} S_{p-1}^{z'} \sin(\theta_p - \theta_{p-1}) = 0, \end{aligned} \quad (9)$$

and we are left with

$$\begin{aligned} H_{\text{eff},p}^{x'} = & 4J_{p,p-1} S_{p-1}^{x'} \cos(\theta_p - \theta_{p-1}) \\ & + 4J_{p,p+1} S_{p+1}^{x'} \cos(\theta_{p+1} - \theta_p). \end{aligned} \quad (10)$$

Equations (7) and (8) remain unchanged. Disregarding second-order terms, we obtain the simplified equations of motion for a canted system:

$$\begin{aligned} -\frac{i\omega}{\gamma} S_p^{x'} = & S_p^y [H_0 \cos \theta_p + 4J_{p,p+1} S_{p+1}^{z'} \cos(\theta_{p+1} - \theta_p) \\ & + 4J_{p,p-1} S_{p-1}^{z'} \cos(\theta_p - \theta_{p-1})] \\ & - S_p^{z'} (4J_{p,p+1} S_{p+1}^y + 4J_{p,p-1} S_{p-1}^y) \end{aligned} \quad (11)$$

and

III. RESULTS

Having covered the matter of calculations and constants, we can return to the qualitative aspects of the system. Keep in mind that the basic configuration of the superlattice resembles a ferrimagnet. While a ferrimagnet is composed of alternating up and down spins, the superlattice examined in this paper is composed of alternating *blocks* of up and down spins. This resemblance is far more than a mere superficial feature of the system. Indeed, some of the most interesting features of the magnon modes can be explained in terms of the ferrimagnet-like structure of the superlattice.

With the above in mind, we briefly review some of the properties of a simple ferrimagnet. The dispersion relation for a bcc ferrimagnet with propagation parallel to a side of the cube is given by

$$\begin{aligned} \frac{\omega^{(\pm)}}{\gamma} = & \pm [4J_I (S_{\text{up}} - S_{\text{down}}) + H_0] \\ & + 4J_I \sqrt{S_{\text{up}}^2 + S_{\text{down}}^2 - 2S_{\text{up}} S_{\text{down}} \cos kL}. \end{aligned} \quad (15)$$

This equation was arrived at using mean-field theory with nearest-neighbors interactions. The derivation is straightforward; an analogous derivation for an antiferromagnet is presented in Ref. 12. Note that increasing the magnetic field simply shifts one mode up and one mode down by a constant amount. For small wave vectors, Eq. (15) may be expanded, with one solution being

$$\frac{\omega}{\gamma} = \frac{2J_I S_{\text{up}} S_{\text{down}}}{(S_{\text{up}} - S_{\text{down}})} (kL)^2 + H_0. \quad (16)$$

Note that at $kL=0$ the frequency is the Larmor frequency γH_0 for precession of a single independent spin in an applied field. Physically this corresponds to all spins being strictly antiparallel to their nearest neighbors so that the exchange field does not produce any contributions to the torque in the Bloch equations.

We now return to the superlattices and consider a system composed of equal layers of *A* and *B* (an n/n system). Such a structure will have $2n$ magnon modes. The $4/4$ system, for instance, has eight modes. We will however only analyze the four lowest modes in any detail since the higher frequency modes are less physically significant due to low thermal occupancy.

We first discuss the spin waves that propagate perpendicular to the layers in a $4/4$ superlattice at $t=0$. With a small applied field, the system will be in the aligned state. The dispersion relation for this case is presented in Fig. 1. In this figure, we see the usual features associated with a periodic structure—bands and band gaps at the zone boundary. There are some slight differences between the general features in Fig. 1 and previous work on ferrimagnetic superlattices with ferromagnetic coupling. In the previous work² there was always a regular alternation between modes with positive group velocity and those with negative group velocity. Here no such simple pattern exists; the first two modes have positive group velocity as does the fourth, while the third mode has a negative group velocity.

It is worthwhile to examine the nature of the modes in Fig. 1 more closely. The spin pattern of a mode can be represented as a vector diagram of the spins in a single unit cell. For instance, at $T=0$, $H_0=0$, and $kL=0$, the modes can be represented as shown in Fig. 2. Such a diagram is simply a snapshot of a unit cell, as viewed from a point on the z axis. The lines drawn through the ends of the spin vectors serve to highlight the magnon wave form. Note that, in general, the higher frequency modes have more nodes in their wave forms, i.e., a shorter wavelength. This is easily understood. Spin waves in a simple

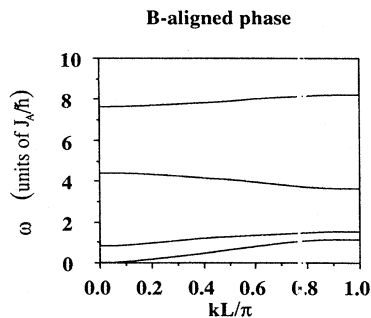


FIG. 1. Dispersion curves for the four lowest modes of the $4/4$ system in the *B*-aligned state. The field $H_0=0$ and the reduced temperature $t=0$. Propagation is along the y axis.

ferromagnet have a dispersion relation of $\omega = Dk^2$ (for k small) where D is the exchange stiffness constant, and the wave vector k is given by $2\pi/\text{wavelength}$. Thus one expects higher frequencies at shorter wavelengths. This general consideration has to be modified somewhat for the superlattice. In our superlattice, the exchange interaction in film *A* is much stronger than that in film *B*; therefore, the stiffness constant is higher in material *A* than in material *B*. Furthermore, the “wavelength” in one material is generally not the same as the “wavelength” in the other material. With the above considerations in mind, we now can investigate the magnon wave forms in some detail. The highest-frequency mode (mode 8) has three nodes in material *A* and only one in material *B*. In comparison, the fifth mode with three nodes in *B* and one in *A* has a much lower frequency. Similarly, the fourth mode (no nodes in the *A* film and two in the *B* film) has a much lower frequency than the seventh mode (two nodes in the *A* film and none in the *B* film). Generally speaking, as the number of nodes increases, the frequency increases. This is especially true for nodes within the *A* film (where D is highest).

Of course, the considerations of the previous paragraph can serve only as a rough guide. For example, the frequencies of the third and sixth modes, which both have one node in each film, are far apart. In this case, the relative amplitudes of the modes within the two different layers are more important for the determination of frequency than the number of nodes. An excitation primarily localized in film *A*, for example, is essentially a mode of a single film of *A* which is weakly coupled to film *B*, i.e., the frequency of the mode in film *A* is far from the frequency of any excitations in film *B* and the spins of film *A* drive the spins of film *B* at an off-resonant frequency. In this case, one expects that the frequency of the superlattice mode should be dependent on the wave-

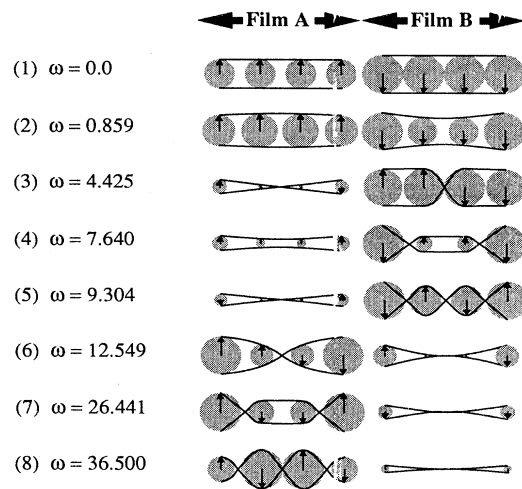


FIG. 2. Spin-vector diagram for all eight modes of the $4/4$ system in the *B*-aligned state. Temperature and external field are set at zero; $k=0$. The ferrimagnetic mode is the first mode. Frequency is given in units of J_A/\hbar .

length and exchange constant in film *A*. Since the sixth mode has a large amplitude in film *A* (the film with the larger exchange constant) while the third mode has a large amplitude in film *B*, the sixth mode has a higher frequency than the third mode. In general, *everything else being equal*, an increase in the number of nodes or a shift in the amplitude from the *B* film to the *A* film will result in an increase in frequency.

An analysis of the magnon wave forms can also be used to explain the field-dependent behavior of a mode. Consider the *B*-aligned state. The dependence of frequency on field strength in this state is simple. The dispersion curves of half of the modes are shifted up by a uniform amount, while the others are shifted down by the same amount. (Specifically, the second, sixth, seventh, and eighth modes decrease with increasing field while the first, second, fourth, and fifth modes increase.) This is again quite reminiscent of the ferrimagnet. Physically, as the external field increases, the effective field in the *A* film *decreases* (since the *A* moments are antiparallel to the field). This effect naturally would tend to reduce the frequency of the superlattice mode. On the other hand, an increase in H_0 *increases* the effective field in the *B* film. This would tend to increase the frequency of the mode. Depending on the particular characteristics of a mode, one of these effects will dominate. If the excitation is primarily localized in the *B* spins, the frequency should go up. Excitations primarily localized in the *A* spins should decrease in frequency as the field is increased. Based on these considerations, we would expect modes 3, 4, and 5 to increase in frequency and modes 6, 7, and 8 to decrease in frequency when a field is applied. This is indeed the result we find. The first two modes are not as clearly localized, but (from Fig. 2) we can see that mode 1 has larger transverse moments in film *B* while, on average, mode 2 has larger transverse moments in film *A*. Thus mode 1 increases and mode 2 decreases in frequency with applied field. Mode 2 is, in fact, driven to zero at a nonzero value of k at $H_0 = 0.8723$ indicating the phase transition from the aligned to the twisted state. This value for the critical field is in agreement with the result found by the iteration method in Ref. 6.

We now turn to the temperature-dependent behavior of the spin-wave modes. This is calculated within the mean-field approximation where the magnitudes of the spins are given by their thermal averaged values found in the self-consistent iterative calculation described in Ref. 6. Thus these results should only provide a general guide to the thermal behavior that is to be expected.

The dispersion curves of the first two modes in the *B*-aligned state (propagation again perpendicular to the layers) at three different temperatures are shown in Fig. 3. A number of interesting features are evident. First, at $kL = 0$, one mode always starts at γH_0 , independent of the temperature. Furthermore, the frequency of this mode (at nonzero values of kL) *increases* with increasing temperature while the frequencies of the other modes *decrease*. An increase in temperature generally results in a decrease in the thermally averaged value for the magnitude of the spins in the system. This, in turn, causes a decrease in the effective fields which then reduces the

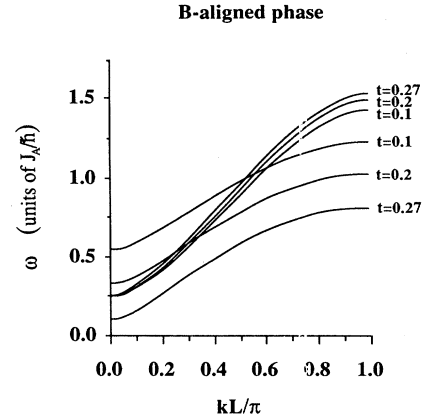


FIG. 3. Dispersion curves for the two lowest modes of the 4/4 system in the *B*-aligned state at three different values of temperature; $H_0 = 0.25$. Propagation is along the *y* axis. The ferrimagnetic mode is temperature independent at $k = 0$, and the frequency increases with temperature at higher values of k .

torque on the individual spins. Therefore, the rate of precession should normally be slower.

The interesting field and temperature dependence of the mode described above can be understood in analogy with a simple ferrimagnet. In the ferrimagnet, one mode has a frequency at $k = 0$ of γH_0 when all the spins are strictly antiparallel to their nearest neighbors. In the superlattice we have seen that there is an analogous mode (top mode in Fig. 2) in which all spins in a film are parallel to the spins within that film but antiparallel to the spins in adjacent films. Thus, each spin is precisely aligned with the exchange field produced by its neighbors. Therefore, the only torque which is present is produced solely by the external field, and the frequency is determined by the external field alone. Thus this mode has a frequency of γH_0 at $kL = 0$. The unusual temperature dependence of this mode at $k \neq 0$ can also be related to its ferrimagnetic nature. Consider Eq. (16) with S_{up} replaced by $S_B(T)$ and S_{down} replaced with $S_A(T)$, i.e., as an approximation replace S_{up} and S_{down} by the bulk, temperature-dependent values for the *A* and *B* spins. The coefficient in front of the $(kL)^2$ term in Eq. (16) then becomes temperature dependent. For example, at $T = 0$ this coefficient is $17.5J_I[S_B(T=0) = \frac{7}{2}$ and $S_A(T=0) = \frac{5}{2}]$. At $T = 200$ K the coefficient is $46.7J_I[S_B(T=200) \approx 2.8$ and $S_A(T=200) \approx \frac{5}{2}]$. Clearly, in this case, the frequency increases as the temperature increases.

Propagation along the *z* and *x* axes (i.e., parallel to the layers) also has a few interesting properties. As in a single magnetic film in the absence of dipolar interactions, there is no difference between magnons travelling in the *x* and *z* directions, either in terms of magnon character or frequency. The field-dependent behavior of the lower modes remains basically the same when the direction of propagation changes from perpendicular to the layers to parallel to the layers. However, temperature-dependent behavior does change slightly. Figure 4 shows the *x*

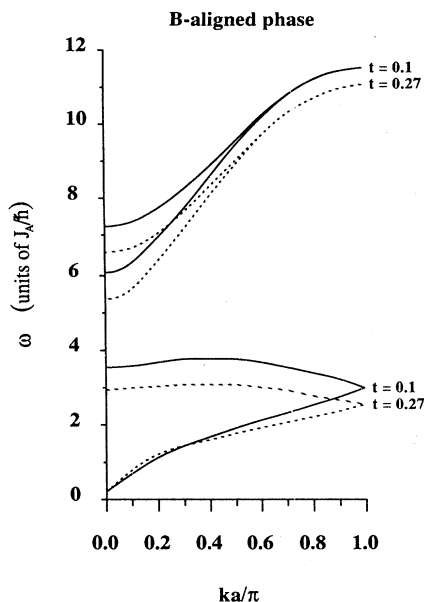


FIG. 4. Dispersion curves for the lowest four modes of the 4/4 system in the *B*-aligned state at $t = 0.1, 0.27$ and $H_0 = 0.25$. Propagation is along the x axis.

direction (z direction) dispersion curves for the first four modes of the 4/4 system at $t = 0.1, 0.27$ and $H_0 = 0.25$. The first mode retains much of its unusual temperature-dependent behavior; careful examination reveals that at low values of ka the ferrimagnetic mode does indeed have higher frequencies at higher temperatures. However, as ka increases, this is no longer true; near the short-wavelength edge of the Brillouin zone the frequency of the ferrimagnetic mode clearly decreases with increasing temperature. This reversal of the temperature-dependent behavior can be explained in terms of the magnon character of this mode. At low values of ka , this mode has the same ferrimagnetic character noted earlier in the discussion of y -travelling magnons; ω is equal to γH_0 at $k = 0$ and the mode strongly resembles its $k = 0$ spin-vector diagram (as shown in Fig. 2). However, as ka increases, the spin wave becomes increasingly localized at the two spins at the center of the *B* film until, at $ka = \pi$, it is confined entirely to these two spins. Thus, near this edge of the Brillouin zone, the spin wave is effectively decoupled from the rest of the superlattice; such a spin wave acts as though it is travelling through bulk *B* material. In other words, at low values of k_x , the mode retains its superlattice nature, but, as k_x increases, the mode loses this character and increasingly resembles a magnon which is travelling through a simple crystal. Therefore, its temperature-dependent behavior will be similar to that of such a magnon; frequency will decrease with increasing temperature.

Interestingly, the ferrimagnetic mode is not the only mode which displays this sort of behavior at $ka = \pi$. In fact, at this end of the Brillouin zone, all the modes are confined entirely to pairs of identical spins (see Fig. 5).

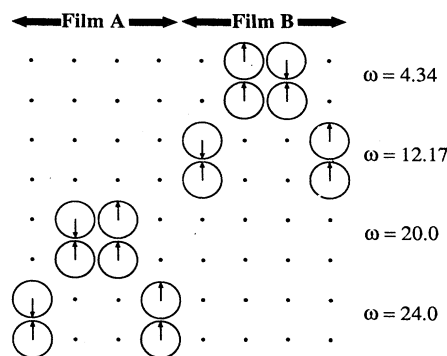


FIG. 5. Spin-vector diagram at $k_x a = \pi$ for all eight modes. The frequency of each degenerate pair at this value of k_x is shown on the right. Frequency is given in units of J_0/\hbar . Both temperature and external field are set at zero.

(These spins are identical in the sense that the static configuration at these lattice sites is identical.) This behavior is reminiscent of the behavior of phonon modes travelling through a diatomic crystal; at the short-wavelength end of the Brillouin zone, displacements are confined entirely to a single sublattice. Note that since there are only four possible pairs of identical spins but eight modes, degeneracy occurs at $kL = \pi$ (see Figs. 4 and 5).

Having dealt with the *B*-aligned phase, let us move on to the twisted state. First, it should be noted that the magnon modes in this state were found to exhibit elliptical rather than circular precession within the *local* (x', y, z') coordinate system. At most values of temperature and field, the ellipticity is slight. Consider the case of the 4/4 system at $t = 0.36$ and $H_0 = 0.125$. At this value of field, the spin configuration resembles a canted state or spin-flop state. Figure 6 is a spin-vector diagram of the second and third modes of this system as viewed in

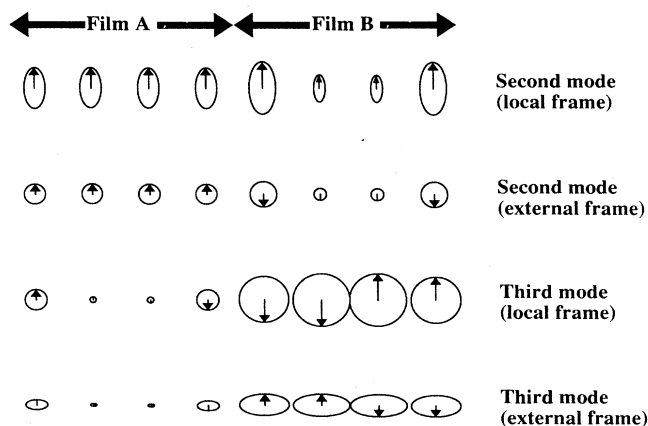


FIG. 6. Spin-vector diagrams at $k_y = 0$ for the second and third modes of the 4/4 system in the twisted state. Each mode is shown as it appears in both the local and external reference frames. $H_0 = 0.125$ and $t = 0.36$.

both the local and the external coordinate systems. Note that the spins of the second mode (the ferrimagnetic mode) exhibit elliptical precession within their local coordinate systems; however, the precession looks circular when projected on the external x - y plane. Thus, this mode, and only this mode, mimics the behavior of an aligned-state mode in the sense that the precession looks circular in the external reference frame. The third mode is representative of the higher modes in the sense that the precession is nearly circular when viewed within the local coordinate system but quite elliptical when projected on the external x - y plane. The ellipticity of the precession is physically very important. For instance, if elliptical precession is present, a change in the polarization of a transverse rf field will result in a change in the rate of power absorption from that field.

As the system enters the twisted phase, a number of other behaviors not seen in the aligned state show up. For instance, as shown in Fig. 7, the lowest mode at $kL=0$ is approximately zero, regardless of the magnitude of the external field. High-resolution analysis reveals that the frequency increases only very slightly with increasing field at these low values of k . At higher values of k this mode is much more strongly field dependent. Helical structures, which bear a superficial resemblance to the canted phase of this superlattice, exhibit similar behavior; that is, at $k=0$, there is a spin wave with frequency zero, regardless of the applied field.¹³ Notice that the ferrimagnetic mode (second mode in Fig. 7) is still present, and its field-dependent behavior is essentially the same as in the B -aligned state.

The frequency of the first mode of Fig. 7 increases with

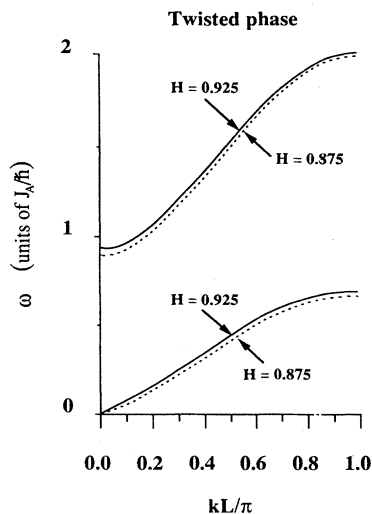


FIG. 7. Dispersion curves for the lowest two modes of the 4/4 system in the twisted state for two different values of external field; $t=0$. Propagation is along the y axis. Note that at $k=0$, the frequency of the lowest mode is approximately independent of the strength of the external field. Note also that the ferrimagnetic mode is present in the canted state and its frequency at $k=0$ is equal to $\omega=\gamma H_0$, where γ is set equal to unity.

increasing temperature at nonzero values of kL as shown in Fig. 8. At $kL=0$, this mode is approximately zero, independent of temperature. At $kL=0$, the ferrimagnetic mode (second mode in Figs. 7 and 8) is still temperature independent. At slightly larger values of kL , frequency decreases with increasing temperature. Thus, the ferrimagnet model breaks down in the twisted state for large values of k .

The aligned state that has been discussed so far is actually the B -aligned state. At high temperatures and low applied fields, the system is in the A -aligned state. The most interesting modes for the 4/4 system in the A -aligned state are the two lowest. The dispersion curves for these modes are shown in Fig. 9. Note that the ferrimagnetic mode is present; the frequency at $kL=0$ is equal to H_0 . The other mode of Fig. 9 also exhibits some interesting field-dependent behavior; the frequency decreases as the external field increases (just as in the B -aligned state). At sufficiently large fields, this mode is driven to zero and a phase transition to the twisted state takes place.

The field-dependent behaviors of the other modes point out an interesting feature of the system as a whole. Note, in the analysis that follows, that the highest six modes have essentially the same character in the A -aligned phase as they had in the B -aligned phase; in other words, the spin-vector diagrams are qualitatively the same. When the system was in the B -aligned state, the frequencies of the three highest modes decreased with increasing

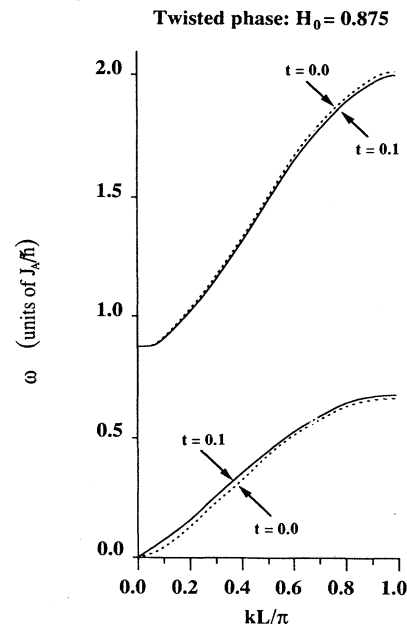


FIG. 8. Dispersion curves for the lowest two modes of the 4/4 system in the twisted state for two different values of temperature; $H_0=0.875$. Propagation is along the y axis. The frequency of the ferrimagnetic mode now decreases as temperature is raised, and the frequency of the other mode increases as temperature increases.

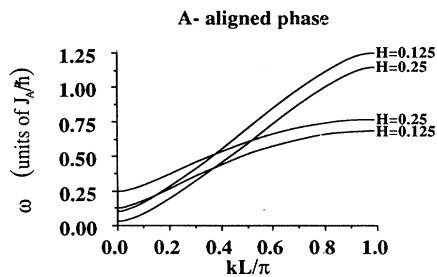


FIG. 9. Dispersion curves for the two lowest modes of the 4/4 system in the *A*-aligned state for two different values of external field; $t=0.4$. Propagation is along the *y* axis.

field while the frequencies of the third, fourth, and fifth modes increased. In the *A*-aligned state, the situation is reversed. When the system is flipped the field-dependent behaviors of these modes also "flip." This should not be too surprising. Recall that the frequencies of the sixth, seventh, and eighth modes in the *B*-aligned state decreased with increasing H_0 because these modes were localized in the film for which the spins were aligned antiparallel with the external field. When the system flips, this film becomes aligned with the external field. Therefore, an increase in H_0 will now result in an increase in the total effective field within this film. Thus, an increase in H_0 will result in an increase in the frequencies of these modes. Similarly, the frequencies of the third, fourth, and fifth modes of the *A*-aligned phase decrease as the external field is increased. Thus, the field-dependent behaviors of the six highest modes flip when the system flips. However, as noted above, the field-dependent behaviors of the two lowest modes do *not* flip when the system flips. This is because the spin patterns of these two modes *do* change when the system is flipped. Therefore, the analysis given above cannot be successfully applied to the two lowest modes.

Although the ferrimagnetic mode retains its usual field-dependent behavior in the *A*-aligned state, its temperature-dependent behavior differs from that exhibited in the other aligned state; the frequency decreases as temperature increases (at nonzero values of k). However, this mode is still temperature independent at $kL=0$ (see Fig. 10). The other mode of Fig. 10 also exhibits some unusual temperature-dependent behavior. For instance, frequency increases with increasing temperature (especially at long wavelengths). At $kL=\pi$, the mode has a much weaker temperature dependence than it has at $k=0$. The higher modes behave in a much more normal fashion; the frequencies of these modes decrease with increasing temperature.

The dynamics of systems with unequal numbers of layers of *A* and *B* are, generally speaking, qualitatively similar to the dynamics of n/n systems, provided that the static configurations are equivalent. The temperature-dependent effects do, however, yield some surprises. In Fig. 11, the dispersion curves for the two lowest modes of the *A*-aligned phase of the 7*A*/5*B* system are shown for three different temperatures. The ferrimagnetic mode is

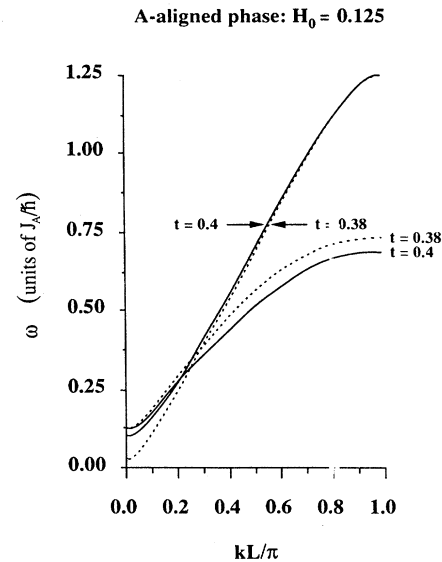


FIG. 10. Dispersion curves for the two lowest modes of the 4/4 system in the *A*-aligned state for two different values of temperature; $H_0=0.125$. Propagation is along the *y* axis. The frequency of the ferrimagnetic mode now decreases as temperature is raised, and the frequency of the other mode increases as temperature increases (especially at long wavelengths).

represented by a dashed line; the frequency of this mode decreases as the temperature increases at $k \neq 0$. The other mode (represented by a solid line) increases with temperature as the temperature is raised from $t=0.2$ to $t=0.4$. Then, as the temperature is further raised from $t=0.4$ to 0.6, the frequency decreases.

IV. CONCLUSION

Using a simple mean-field approximation with nearest-neighbor interactions only, we have calculated the spin-wave spectrum for a system composed of alternating films of two ferromagnetic materials (referred to as materials *A* and *B*). Although the materials themselves are ferromagnetic, the interaction at the interfaces between

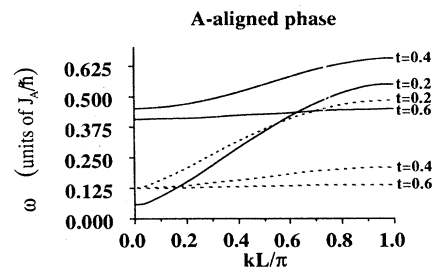


FIG. 11. Dispersion curves for the two lowest modes of the 7/5 system in the *A*-aligned state for three different values of temperature; $H_0=0.125$. Propagation is along the *y* axis. The ferrimagnetic mode is represented by a dashed line. Note that the ferrimagnetic mode is temperature independent at $k=0$.

these two materials is antiferromagnetic. At $t=0$, material A has a moment of $\frac{5}{2}$ while material B has a moment of $\frac{7}{2}$. Material B has a much lower Curie temperature than material A . Such a system can, depending on the temperature and the magnitude of an externally applied magnetic field, exist in any of four distinct phases (A -aligned, twisted, B -aligned, and paramagnetic). The paramagnetic phase exists only at extremely high values of temperature and field and, therefore, was neglected.

We examined the frequency of the spin waves in this structure as a function of the temperature and the magnitude of the applied field. Several unusual temperature- and field-dependent behaviors were discovered. Magnons travelling in the y direction (perpendicular to the interfaces) through a $4/4$ system in the A -aligned phase were discussed first. The frequency of one of the modes in this phase is independent of temperature at $k=0$ and is equal to γH_0 . At higher values of k , the frequency of this same mode increases as the temperature increases; normally one would expect just the opposite. Both behaviors can be explained in terms of an analogy with a simple ferrimagnet. The temperature-dependent behaviors of the other modes are much more conventional; frequency decreases as temperature increases. Half the modes showed an increase in frequency as the external field increased, and half showed a decrease. The field-dependent behavior of the modes can be explained in terms of the spin patterns associated with each mode.

Propagation parallel to the film interfaces was also analyzed. At short wavelengths the frequency of the ferrimagnetic mode decreased as temperature increased. At long wavelengths, the frequency of this mode increased as temperature increased. This reversal in the temperature-dependent behavior can be related to the magnon spin

pattern at $k_{x(z)}a=\pi$. At this end of the Brillouin zone, all the modes are confined entirely to pairs of identical spins.

In the twisted state, the frequency of the ferrimagnet-like mode decreases with increasing temperature (in stark contrast with its behavior in the B -aligned phase). Note that, in this state, the spins precess elliptically. The twisted state is also marked by the appearance of a mode which is approximately field and temperature independent at $k=0$. At higher values of k , the frequency of this mode increases as temperature increases.

In the A -aligned phase, the field-dependent behaviors of several of the modes reverse. This reversal can be explained in terms of magnon character. The ferrimagnetic mode retains its characteristic temperature and field dependent behavior at $k=0$. However, at nonzero values of k , the frequency of this mode decreases as temperature increases. The behavior of the spin-wave modes in systems which have unequal numbers of layers of A and B is qualitatively similar to the behavior of n/n system modes.

Certain features of the system, such as the dependence of the frequency on the external field, can be explained in terms of the ferrimagnet-like structure of the superlattice and the characteristics of individual modes. Furthermore, an examination of the eigenvectors of a mode can be used to determine its relative frequency (with respect to the frequencies of the other modes).

ACKNOWLEDGMENTS

This work was supported by the U. S. Army Research Office under Grant No. DAAL03-88-K-0061.

¹L. Esaki and R. Tsu, IBM J. Res. Dev. **14**, 61 (1970).

²E. L. Albuquerque, P. Fulco, E. Sarmiento, and D. P. Tilley, Solid State Commun. **58**, 41 (1986); F. Fishman, F. Schwabl, and D. Shwenk, Phys. Lett. A **121**, 192 (1987); R. E. Camley, B. Martinez, and J. G. LePage, J. Phys. (Paris) Colloq. **C8**, 1691 (1988).

³L. L. Hinchey and D. L. Mills, Phys. Rev. B **33**, 3329 (1986); **34**, 1689 (1986).

⁴D. J. Webb, A. F. Marshall, A. M. Toxen, T. H. Geballe, and R. M. White, IEEE Trans. Magn. **24**, 2013 (1988); D. J. Webb, R. G. Walmsey, K. Parvin, P. H. Dickenson, T. H. Geballe, and R. M. White, Phys. Rev. B **32**, 4667 (1985).

⁵P. Grunberg, R. Schreiber, Y. Pang, M. B. Brodsky, and H. Sowers, Phys. Rev. Lett. **57**, 2442 (1987); C. Carbone and S. F. Alverado, Phys. Rev. B **36**, 2433 (1987).

⁶J. Krebs, C. Vittoria, B. T. Jonker, and G. A. Prinz, J. Magn. Mater. **54-57**, 811 (1986).

⁷J. Kwo, E. M. Gyorgy, D. B. McWhan, M. Hong, F. J. DiSal-

vo, C. Vettier, and J. E. Bower, Phys. Rev. Lett. **55**, 1402 (1985); C. F. Majkrzak, J. W. Cable, J. Kwo, M. Hong, D. B. McWhan, Y. Yafet, and J. V. Waszczak, *ibid.* **56**, 2700 (1986).

⁸M. Taborrelli, R. Allenspach, G. Boffa, and M. Landolt, Phys. Rev. Lett. **56**, 2869 (1986).

⁹See, for example, K. Moorjani and J. M. D. Coey, *Magnetic Glasses* (Elsevier, Amsterdam, 1984), Chap. VI.

¹⁰R. E. Camley and D. R. Tilley, Phys. Rev. B **37**, 3413 (1988); R. E. Camley, *ibid.* **39**, 12316 (1989).

¹¹S. Tsunashima, T. Ichikawa, M. Nawata, and S. Uchiyama, in Proceedings of the International Conference on Magnetism, Paris, 1988, [J. Phys. (Paris) Colloq. **C8**, 1803 (1988)]. For transitions between various aligned states see D. J. Webb, R. G. Walmsey, K. Parvin, P. H. Dickenson, T. H. Geballe, and R. M. White, Phys. Rev. B **32**, 4667 (1985).

¹²C. Kittel, *Introduction to Solid State Physics* (Wiley, New York, 1986), Chap. 15.

¹³B. R. Cooper, Solid State Phys. **21**, 447 (1968).